Temperature dependence of exciton resonances, in monolayer WS_2

Bas Tuin
12855588

June 29, 2022

Study	Bachelor thesis Physics and Astronomy (15 EC)
	Conducted between 4-4-2022 and 29-06-2022
Supervisor	Jorik van de Groep
Daily supervisor	Ludovica Guernéri
Examiner	Anna Isaeva
Institute	Van der Waals-Zeeman Institute, Institute of Physics
University	Universiteit van Amsterdam
Faculty	Faculteit der Natuurwetenschappen, Wiskunde en Informatica

Abstract

We performed photoluminescence (PL) measurements on monolayer WS_2 at different temperatures between 293 K and 83 K to study the PL energy shifts as function of temperature for both excitons and trions. Before taking low temperature measurements we first characterized the material at room temperature using PL, Raman and reflectance spectroscopy. We find that the PL peak position is well described by the Varshni equation, but with different constants then for a 3D crystal. Although the general trends matched with theory, for unknown reasons the low temperature measurements showed unusually low intensities when compared to the room temperature characterization measurements. Although we suspect this to be caused by the sample moving in the cryostat we do not know for certain. Besides this we also believe this to have caused the Full Width Half Max measurements to not match theory.

Contents

1 Introduction

2D Transition metal dichalcogenides (TMD) are a type of semi-conductor that have recently gained popularity. This is because they have unique optical and electrical properties as a result of their layered structure. Examples include strong tuneable light-matter interactions in the visible spectral range, despite being atomically thin due to having a direct band gap with a size that is very useful for solar panels [1]. The solar cells made of 2D TMDs are particularly promising since they could allow for cheaper, thinner, and more flexible solar panels.

The optical properties of 2D TMDs are mostly dominated by excitons, which are quasi-particles that consist of an electron and hole in a bound state. The radiative recombination of excitons dominates the photoluminescence (PL) spectrum of the monolayer TMDs.

The optical response of the material is also affected by phonons which are quasi-particles that represent lattice vibrations which cause peak broadening and redshift of the PL spectra. Because the phonon occupation is reduced when temperature decreases, we expect the PL spectra to become narrower and blueshift with lower temperature. Because of this temperature dependence the optical properties of the TMD monolayers also change with temperature, which will also affect the performance as well as the functional spectral range of the WS_2 solar cell. Therefore, to study these effects we pose the following research question *"What is the temperature dependence of the exciton resonances in monolayer WS_2"*.
Here, we perform low-temperature optical spectroscopy to study the temperature dependence of high-quality exfoliated monolayers of WS2. We find that the exciton energy shows a monotonic blue shift, in accordance with theory. However, experimental complications hinder the quantitative analysis of the PL results to characterize phonon interactions.

1.1 Outline

This thesis has the following structure. In chapter 2 we describe the properties of transition metal dichalcogenides, excitons and phonons, we also describe how we perform photoluminescence, Raman and reflectence measurements. After this we describe the process of sample fabrication, as well as the experimental setup for both the characterization and low temperature measurements in chapter 3. Next we show the results, discuss their interpretations and compare the results to theory in chapter 4. In chapter 5 we will discuss the potential improvements of this experiment and how they affect the results. Finally in chapter 6 we conclude the thesis and give an outlook for further experiments.

2 Theory

2.1 Transition Metal Dichalcogenides

Transition metal dichalcogenides (TMDs) are semiconductors with the structure MX_2 with M being a transition metal such as Molybdenum (Mo) or tungsten (W), and X being a chalcogen atom such as Sulfur (S) or Selenide (Se). In these materials the transition metal is bonded to the chalcogen atoms (see figure 1). The stacked monolayers that make up the material are connected by van der Waals forces and therefore have different characteristics then the monolayers solely which can be used to detect the number of layers. The relatively weak van der Waals forces enable exfoliation of layers from the bulk crystal. The electron wavefunctions are quantum confined to the individual layers, and in the limit of a single monolayer the indirect bandgap transitions into a direct bandgap [2]. This is because in reciprocal space the electrons can only stay in the upper region between the K and Γ point if they have a significantly higher energy, which means that the direct bandgap becomes the lowest energy option for electron transitions (see figure 2) [3]. The difference between these types of bandgap is that the indirect bandgap requires a phonon to absorb photons. An electron at the top of the valence band requires both energy and momentum to reach the lowest point of the conduction band, and a photon only gives energy to the electron. To ensure energy and momentum conservation it becomes necessary for the electron to absorb a phonon to gain the necessary momentum. This extra step causes the photon absorption to be slower and it also makes it more difficult for electrons to fall back to the valence band [4]. Monolayer TMDs thus exhibit stronger absorption and brighter photoluminescence signals than their bulk counterpart.

2.2 Excitons

When electrons get excited and move from the valence band to the conduction band they leave behind a hole, which is a positively charged quantum particle. Because the electron and hole have an opposite charge they have a Coulomb attraction. It is possible for the electron and hole to stick together in a bound state that forms a new quasi-particle that is called an exciton. This bound state has a lower energy than the free particle bandgap energy, which causes the bandgap to effectively become smaller by an amount of energy equal to the binding energy (see figure 3). When the electron and hole of an exciton recombine it will emit a photon, which will have lower energy then the bandgap

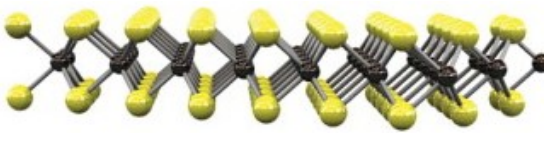

Figure 1: Structure of a monolayer Transition Metal Dichalcogenide as seen from the side, with the black dots representing the transition metal atoms (M) and the yellow dots representing the chalcogen atoms (X) [5].

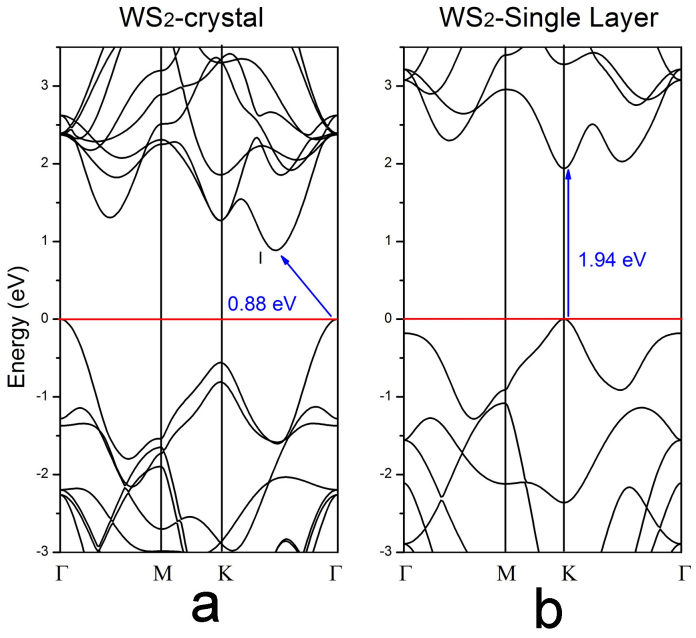

Figure 2: Bandgap for WS_2 for a bulk crystal with a indirect bandgap (a) and for monolayer with a direct bandgap (b) [3].

energy.
Excitons in TMDs can be stable at room temperature because the materials are quantum confined by restricting them to 2D layers, which causes a strong Coulomb interaction and because there are less atoms to screen the Coulomb interaction. This also makes it possible to tune the light-matter interactions by changing the voltage on the material [6].
There are two exciton states for WS_2 called the A and B exciton, due to spin-orbit coupling, which splits the valence band. The low-energy transition is called the A exciton, whereas the higher energy transition is called the B exciton [7]
To measure excitons we shine a laser with sufficient photon energy on the material to create excitons and induce photoluminesence, which will cause a peak to appear at the exciton wavelength.
Besides excitons the material also contains trions, which have one more electron or hole compared to exciton. Because these trions contain three particles it means that they have a larger binding energy compared to excitons and their peak therefore has a lower energy than the exciton peak [8]. Trion peaks are smaller then exciton peaks, because trions usually recombine non-radiatively.

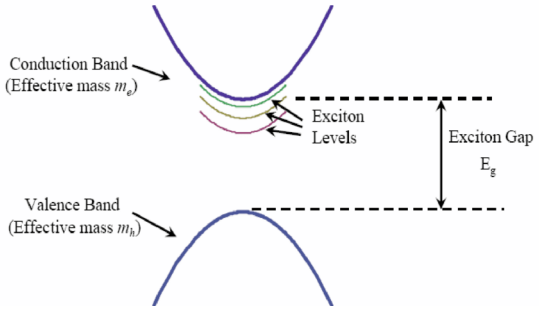

Figure 3: Bandgap with a lowered effective conduction band due to the exciton binding energy [9].

2.3 Photoluminescence

Photoluminescence (PL) occurs when an electron gets excited by a photon with a higher energy than the bandgap. This electron will then quickly lose energy and momentum by sending out phonons until it reaches the bottom of the conduction band, at which point it falls back to the valence band and recombines radiatively with a hole and sends out a photon (see figure 4a). The process of falling back to the valence takes longer than the relaxation by phonons which causes a density of states distribution to form for both the electrons and holes (see figure 4b). It is also possible for the exciton to recombine non-radiatively which does not contribute to the PL spectrum. We fit the PL using a double lorentzian distribution because there are two peaks caused by the exciton and trion respectively, which each have a lorentzian distribution.

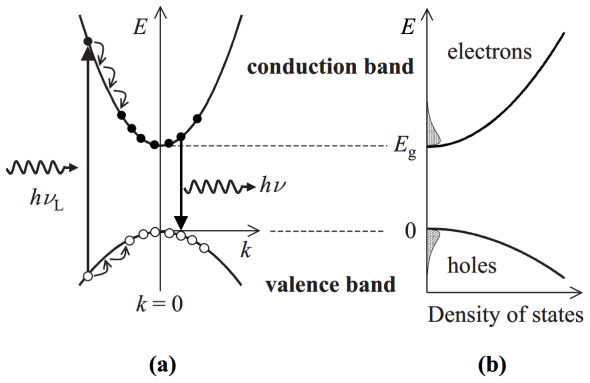

Figure 4: Photoluminescence illustrated for a direct bandgap (a) and the density of states for the bandgap (b) [4]. Note that excitonic effects are ommitted in this schematic

2.4 Raman spectroscopy

Another characterization method we use is Raman spectroscopy that measures Raman scattering. This occurs when the material absorbs light from the laser and excites to a virtual energy state and then immediately falls back to an energy state that is either higher or lower than the original energy state (see figure 5). This shift in energy is caused by phonons with each phonon mode causing a different energy shift, which is why Raman spectroscopy is used to measure phonon modes. Each material has distinctly different Raman peaks for the phonon modes, so that we can make sure that we are using WS_2 on a Si/SiO_2 substrate.
Raman scattering is a form of inelastic scattering as opposed to Rayleigh scattering where the photon energy remains the same [10]. Because of this inelastic scattering there is a shift in the energy of the scattered photons with respect to the incident spectrum, which is usually measured in units of cm^{-1}.

2.5 Reflection spectroscopy

Because Raman spectroscopy cannot measure excitons and PL spectroscopy only measures excitons in monolayers, we decided to also measure the reflectance of the sample to characterize the material. By shining a halogen lamp on the material it will reflect a portion of the light called the spectral radiant flux which we count and compare to a reference mirror. The resulting reflectance is calculated with the following formula

$$R = \frac{\text{Spectral radiant flux} - \text{Dark counts}}{\text{Mirror} - \text{Dark counts}} \times R_{Theoretical}. \tag{1}$$

Here the $R_{Theoretical}$ is used a reference to eliminate system response and the dark counts are the residual counts measured when the laser is turned off. Besides this we can also calculate the differential reflectance by comparing the sample to the substrate using

$$\Delta R = \frac{\text{Spectral radiant flux} - \text{Substrate}}{\text{Substrate} - \text{Dark counts}}. \tag{2}$$

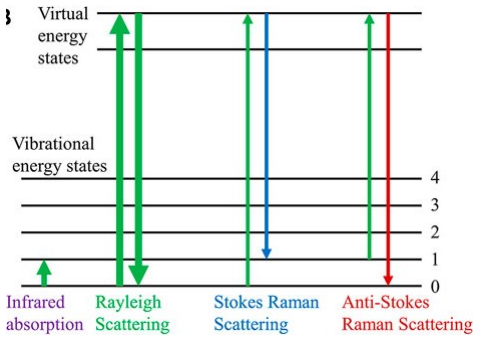

Figure 5: Energy graph comparing Raman scattering to Rayleigh scattering [11].

This differential reflectance divides the contribution to the reflectance of the substrate out of the signal so that the contribution of the sample becomes more apparent.

2.6 Phonons

Phonons are quantummechanical quasi-particles that represent lattice vibrations, which can alter light emission by scattering of excitons, such that it sends out a photon with a different energy than in the absence of phonons. This means that any PL peak will be broadened by phonons. The peak broadening Γ is given by the following formula due to the Fröhlich interaction [12]

$$\Gamma(T) = \Gamma_0 + \sigma T + \gamma < n >, \tag{3}$$

where Γ_0 is caused by inhomogeneous temperature independent broadening, $< n >$ is the average number of phonons and σ and γ are constants for the interaction between excitons and acoustic and longitudonal optical phonons respectively.
Lattice vibrations also cause the average distance between atoms to increase which causes the interaction between neighboring atoms to weaken so that the band gap shrinks which causes the PL to redshift [13].
There are 2 phonon distinctions which form 4 phonon modes. The first distinction is optical and acoustic where, the frequency of the phonon determines if the phonon interacts with light (optical) or with sound (acoustic). The second distinction is longitudinal or transverse which is dependent on the wave vector of the phonon.

There are less phonons at lower temperatures because the lattice vibrations that make up the phonons are caused thermal energy being transformed into vibrational energy. The average phonon occupation number follows Bose-Einstein statistics, and is therefore given by

$$< n >= (e^{\frac{E_g}{k_b T}} - 1)^{-1}, \tag{4}$$

where E_g is the bandgap energy and k_b is the Boltzmann constant This means that the PL spectrum becomes narrower and blueshifts more as the temperature drops.

The phonons cause the exciton PL peak to redshift, which is what we are measuring in this experiment. We expect the excitons peak position to shift according to the Varshni equation [14], which is an empirical formula that assumes that the exciton binding energy is temperature independent.

$$E(T) = E_0 - \alpha T^2/(T + \beta), \tag{5}$$

where E_0 is the energy at $T = 0$ K and α is the constant for the linear part of the equation and β is the constant for the quadratic part if the equation.

3 Methods

3.1 Preparing the material

To make a monolayer WS_2 flake we use tape to peel one layer of atoms from a TMD bulk crystal. We then use a PDMS stamp to place the monolayer on a SiO_2/Si substrate, using a stamping device to precisely control the PDMS position. To make sure the PDMS lets go off the material we use a heating stage that is attached to the sample stage. After heating the material to 323 K we peel the PDMS off very slowly while using the camera to make sure that the material doesn't get peeled off. To check if the material is a monolayer, fewlayer, or bulk we take PL measurements because the monolayer will have much higher PL. We also take Raman and reflectance measurements to make sure that we are dealing with WS_2 on a Si/SiO_2 substrate, which we then compare to theory.

3.2 Optical microscope setup

To perform these measurements, we use the setup shown in figure 6. For the PL and Raman measurements we shine a 532 nm laser with an approximate power of 5μW on the sample which lays on the sample stage. For the reflectance measurements we use a halogen lamp. To observe and locate the sample we use the camera as well as the Witec microscope, where the microscope has different magnifications, but we used a objective with a 50 x magnification. The laser incoupler receives the laser light through an optical fiber and sends it to the sample. The incoupler also separates the reflected laser light from the PL signal using a dicroidic mirror. The outcoupler receives the signal and sends it to the spectograph, which analyses it. To take measurements we close the camera to make sure that the entire signal reaches the outcoupler and if we want to measure the dark counts then we also block the laser.

3.3 Low temperature setup

For the low temperature measurements we replace the sample stage with a Linkam cryostage (see figure 7). The sample is located in a circular chamber covered by a glass plate with liquid nitrogen flowing in the cryostage next to the sample. Using both the heating stage that is attached to the sample stage and the liquid nitrogen flow allows us to precisely control the temperature of the sample. Using liquid nitrogen allows us to lower the temperature of the sample to 83 K. To create a vacuum inside the cryostage we attach a vacuumpump, which creates a vacuum with a pressure between $6 * 10^7$ mbar and $8 * 10^7$ mbar. This sample stage also has pressure and temperature detectors to make sure that the conditions in the vacuum stay the same.
Despite using the vacuum pump it was still possible for air to leak into the vacuum chamber which would then get pumped out the chamber. This leakage is what causes the pressure to fluctuate.

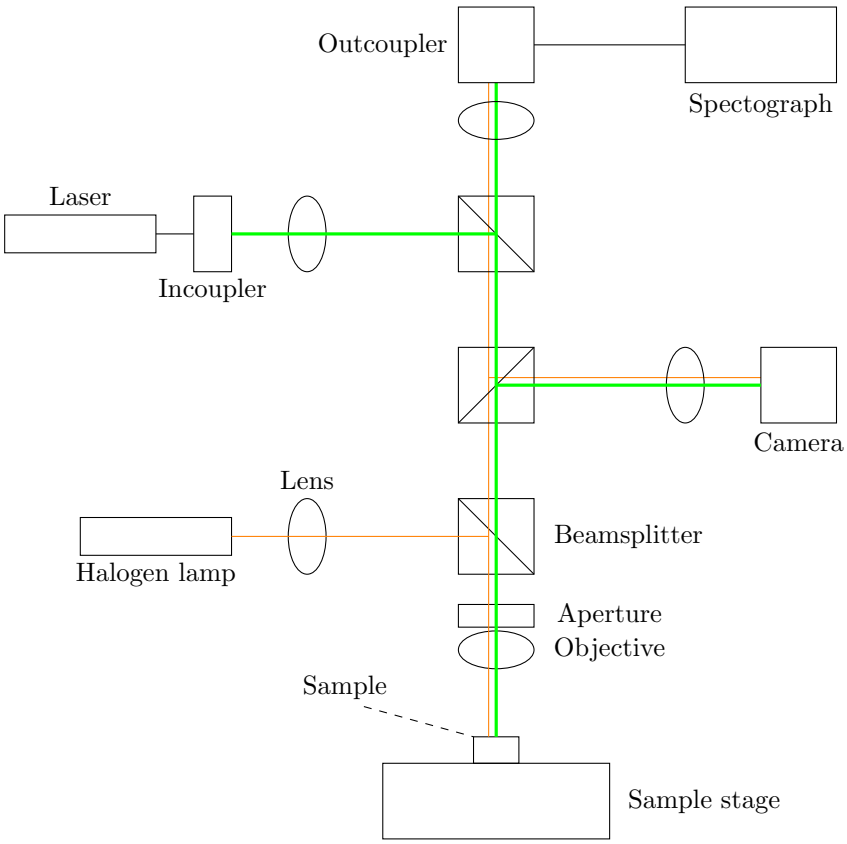

Figure 6: Microscope setup, with the laser in green and the light from the halogen lamp in orange

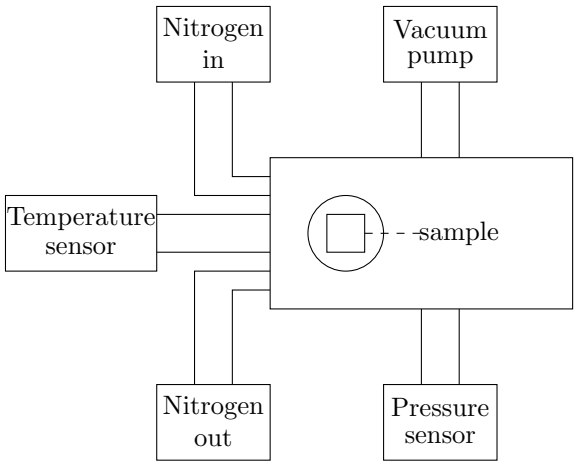

Figure 7: Cryostage for the low temperature measurements with sample in the middle under a glass plate.

4 Results

4.1 Sample preparation

After stamping the WS_2, we were left with a sample that contained a small piece of monolayer, which can be seen in figure 8a highlighted in the red box. To check if the monolayer has uniform thickness we made a PL map by taking a PL spectrum at multiple locations uniformly spaced over a square area and detecting the PL peaks and integrating over the range around it (see figure 8b). On this PL map there is a line which has a higher intensity than the rest of the area which is caused by a wrinkle in the monolayer. Although this monolayer is not perfectly flat, it does have a large enough flat area for the measurements.

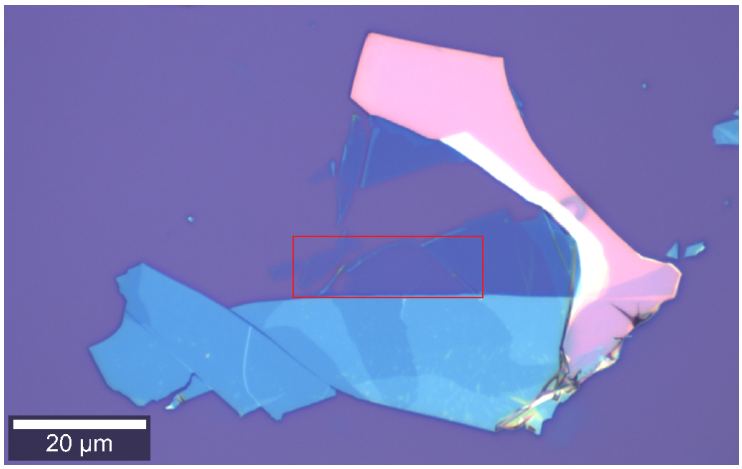

(a)

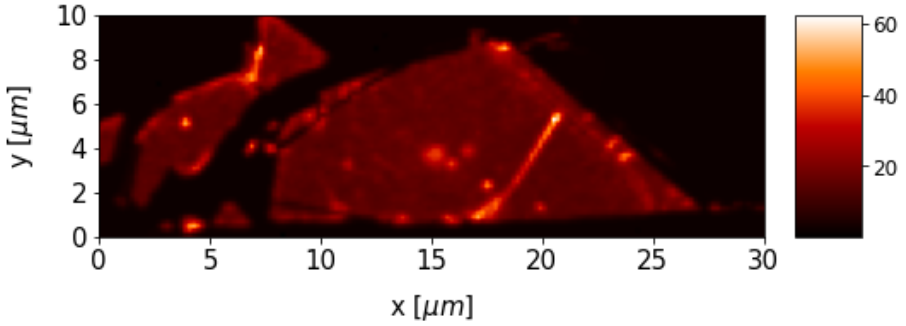

(b)

Figure 8: Sample of WS_2 used for experiment, (a) picture, (b) map of the PL intensity

4.2 Raman spectrum

To ensure that the sample is WS_2 we take Raman spectra. The Raman spectrum has many peaks (see figure 9a), but the two largest peaks are at 353.1 cm^{-1} and at 519.8 cm^{-1}. The first peak is caused by the WS_2 monolayer and the second smaller peak is caused by the Si/SiO_2 substrate, this can be seen when we take a reference spectrum of the substrate. When comparing the monolayer spectrum with the fewlayer and the bulklayer we see that the fewlayer has a higher peak than the monolayer and that the bulk has a peak with similar intensity as the monolayer.
The measured data corresponds to theory which says that the monolayer has a peak at 352.1 cm^{-1} and the substrate has a peak at 520 cm^{-1} [15], it was also expected that the fewlayer peak has a higher intensity than the monolayer peak (see figure 9b). According to theory this monolayer peak is the E^1_{2g} peak which is caused by longitudonal optical phonons. Although theory also dictates that the peak energy shifts between monolayer and bulk, but we did not observe this. These results confirm that the sample is a WS_2 monolayer.

4.3 Photoluminescence characterisation

To characterize the excitons we take PL measurements at room temperature, which are shown in figure 10. This graph shows two peaks, which are caused by excitons and trions respectively with the larger one belonging to the excitons. Fitting this graph with a double lorentzian shows that the monolayer has a exciton peak at 2.02 eV with an Full Width Half Max(FWHM) of 26.7 meV and that the trion peak has an energy of 1.98 eV and a FWHM of 61.1 meV. This corresponds closely to the theory which says that the exciton peak is at 2.017 eV [16].

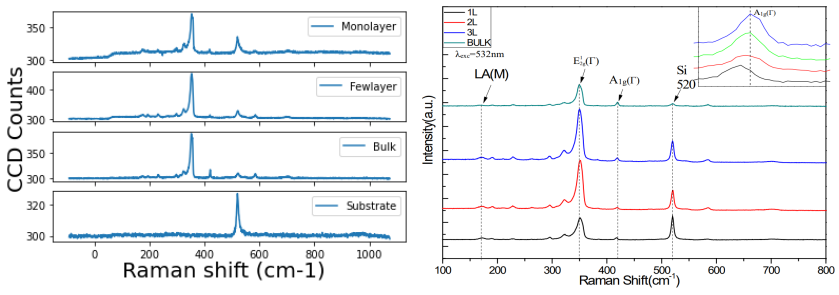

(a) (b)

Figure 9: Raman spectra used for characterisation of the monolayer WS_2 (a) and theoretical spectra to compare it to (b) [15].

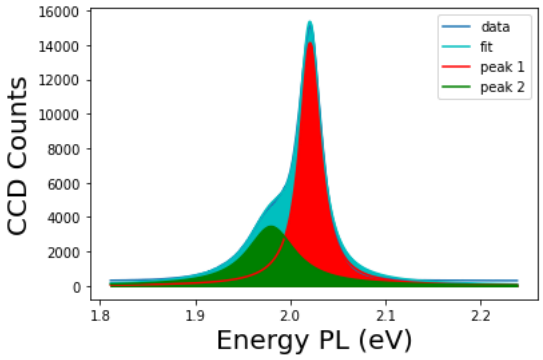

Figure 10: PL spectrum of monolayer WS_2 taken at room temperature.

4.4 Reflection spectrum

Since the bulk material doesn't show PL we take reflection spectra to study excitons. The reflection spectrum is shown in figure 11a and has only one minimum at 2.025 eV for the monolayer and fewlayer but has multiple in the bulk. The differential reflectance is shown in figure 11b and also has one minimum at 2.025 eV for mono- and fewlayer while the bulk is again more complex. In both these graphs the monolayer minimum is deeper and shifted when compared to the fewlayer, which makes sense since the excitons have stronger effect in monolayers.
The reflectance in the measurements looks very different from the theory (see figure 11c) [17], where there are two exciton minima for the A and B exciton and a third minimum C exciton coming from optical transitions. The differential reflectance also shows three peaks for the A, B and C excitons (see figure 11d) [18].
These differences are most likely caused by us using a different substrate than the theory measurements, which caused the reflectance of the B and C exciton to have a low intensity to the point that they aren't distinguishable. To check this we made a calculation of the reflectance of WS_2 and the substrate (see figure 12) using a transfer matrix method, which calculates solutions to the Maxwell equations in a stack consisting of a semi-infinite amount of air, monolayer WS_2 (0.618 nm), 90 nm Si and a semi-infinite layer of Si in that order.
The reflectance theory states that the A exciton sends out photons with a wavelength of $\lambda = 621$ nm, which corresponds to an exciton energy of 1.997 eV while the differential reflectance theory states that the A exciton for monolayer WS_2 has an energy of 2.025 eV. These results indicate that our sample is indeed a WS_2 monolayer even though we couldn't measure the B and C exciton.

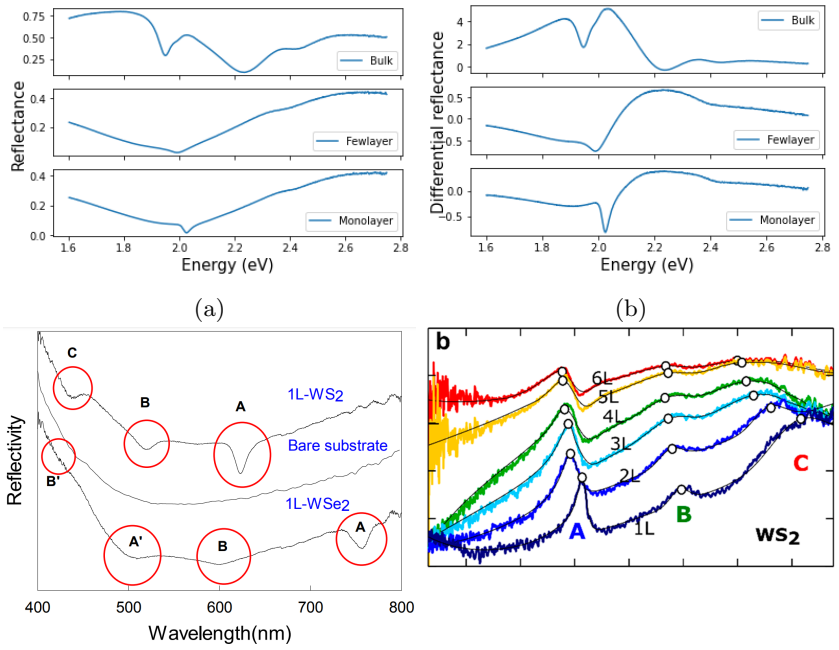

Figure 11: Reflectance and differential reflectance measurements (upper row/a,b) and theory (lower row/c,d) [17]. Picture d has an eV x-axis in eV but this was not shown in the graph[18].

4.5 Low temperature measurements

The low temperature measurements were taken between $T = 293$ K and $T = 83$ K under vacuum. The results of these measurements can be seen in figure 13, where we we can see that the exciton peaks have a significantly lower amplitude then during the characterization measurements while the trion peaks now have a larger amplitude then the exciton peaks. This does not match theory since excitons have a lower binding energy than trions and are therefore easier to recombine and thus should have a higher peak.

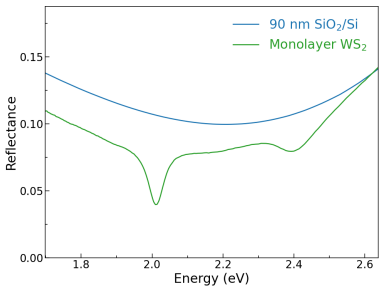

Figure 12: Calculated reflectance of WS_2 monolayer and the substrate, using TMM method.

We can see that the trion peaks become larger at lower temperatures as expected with exceptions at 173 K and 273 K (see figure 14c, 14d). Both peaks at both $T = 173$ K and $T = 273$ K are significantly smaller than expected. While we suspect this to be caused by not focusing on the material properly we do not know for certain if this is the cause. We also see that the exciton peak remains at a small amplitude but still blueshifts. We fit each of the peaks with double lorentzians and plotted their spectral center in figure 14a for the excitons and figure 14b for the trions, which we then fitted using equation 5. The fitting result parameters are shown in table 1).
While the position of the data points roughly follows the expected shape, we see that two of the exciton datapoints have a unexpectedly large error bar. These results show that the uncertainty for β is bigger than its value, which we believe is caused by the fit being mostly linear and having a very small quadratic component, which β is responsible for. This makes it difficult to determine β accurately for both excitons and trions.
The results also show that the excitons have a smaller uncertainty than the trions.
In addition to the energy and intensity of the peaks we also determined their Full Width Half Max (FWHM), which can be seen in figures 14e and 14f as well as their fittings according to equation 3. The results of these fittings is shown in table 2. These figures and results show that the fitting did not work very well, since the graphs show the fittings as straight lines when an exponential function was used, besides this γ and E_g have values of 1 and no standard deviation could be determined. This is most likely caused by the peaks being unnaturally broadened after being placed in the cryostage, which caused the width data to deviate significantly from the expected results.

	exciton	trion
E_0 (eV)	$2.116 \pm 2.377 \times 10^{-2}$	$2.038 \pm 4.012 \times 10^{-3}$
α (J/K)	$3.815 \times 10^{-4} \pm 6.017 \times 10^{-5}$	$3.374 \times 10^{-3} \pm 3.240 \times 10^{-2}$
β (K)	65.62 ± 149.5	$4.327 \times 10^{3} \pm 4.416 \times 10^{4}$

Table 1: Results of the low temperature exciton energy fitting

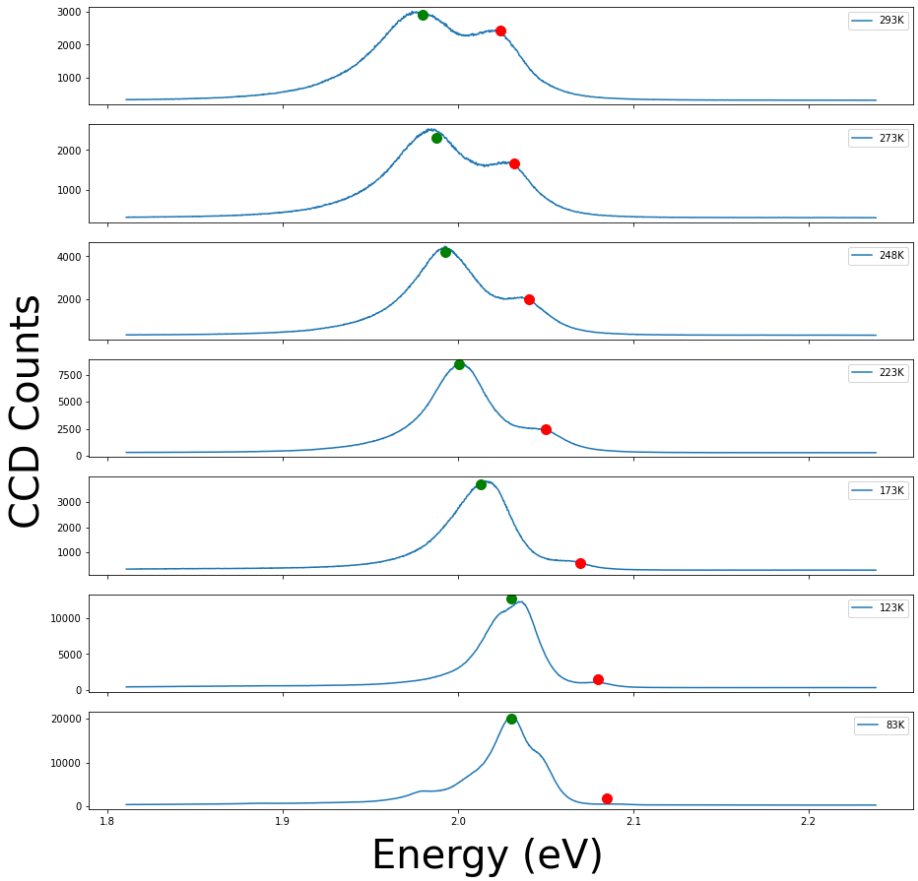

Figure 13: PL of monolayer WS_2 at low temperatures. Red dots represent exciton peak positions while green dots represent trion peak positions, as extracted from fits to the spectra

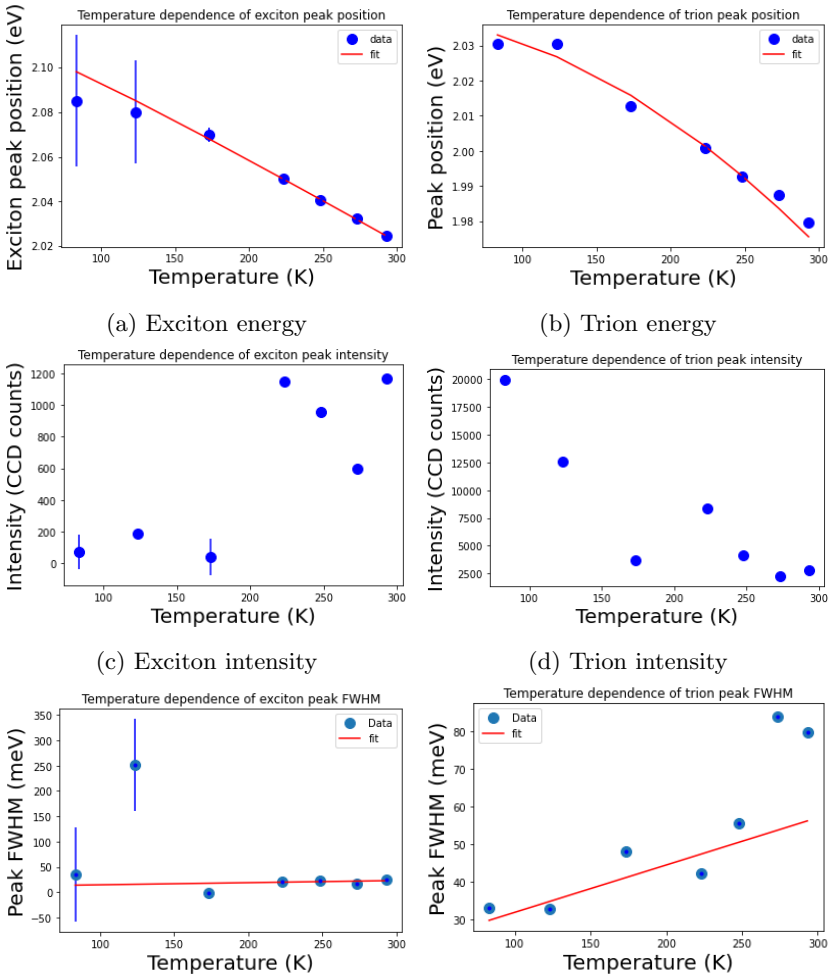

(a) Exciton energy

(b) Trion energy

(c) Exciton intensity

(d) Trion intensity

(e) Exciton FWHM

(f) Trion FWHM

Figure 14: Temperature dependence of the exciton peaks on the left (a,c,e) and the trion peaks on the right (b,d,f). The first row (a,b) shows the energies of the peaks, the second row (c,d) shows the amplitudes of the peaks and the third row (e,f) shows the FWHM of the peaks

	exciton	trion
Γ_0 (meV)	10.32	19.20
σ (meV/K)	4.206×10^{-2}	0.1260
γ	1	1
E_g (eV)	1	1

Table 2: Results of the Full Width Half Max fitting

5 Discussion

The low temperature measurements showed exciton peaks which were much smaller than the characterization measurements (see figure 15a). While we originally suspected sample degradation to be the cause, measuring after taking the sample out of the cryostat revealed this to be false (See figure 15b). Although the exciton peak is smaller then before due to lower laser power, we can still see that the general trends of the spectrum match theory. This means that the environment in the cryostat caused the excitons to recombine non-radiatively, although we currently have no idea why that is.

While equations 3 and 5 are typically used for 3D semiconductors we believe that they can also be used for 2D semiconductors, because the constants used in these equations are not derived from principles but rather emperically determined. This means that these equations can be used if they properly describe the data.

The low temperature measurements had a larger uncertainty than the initial room temperature measurements because the sample often moved slightly inside the cryostat. To prevent the sample from moving we needed to measure for short amounts of time which means that there were less accumulations and resulted in a lower signal to noise ratio. Besides this, we also noticed that after measuring at low temperatures for a long time that small clumps would form on the material (see figure 16). Although baking the sample gets rid of these clumps, it is still possible for them to interfere with the measurements. We are not certain what these clumps are or what causes them, but we suspect that it is caused by air and water entering the vacuum and then slowly freezing. The amount of material that leaked into the vacuum is most likely very small and will therefore not affect the measurements much if we bake away the clumps.

Although the low temperature PL fittings often have an uncertainty that is larger than the value this does not mean that the results are not valid. Since they match with both theory and data and there is a reason for those large uncertainties. The FWHM fittings on the other hand do not match with theory and are unexpected due to unnatural broadening caused by empirical difficulties.

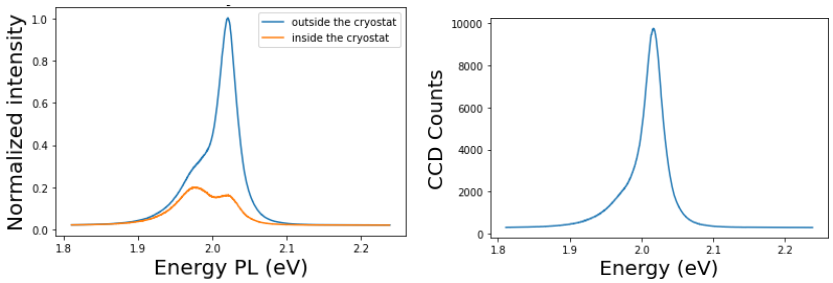

(a) (b)

Figure 15: PL spectra taken at room temperature both inside and outside the cryo stat (a). PL spectra of monolayer WS_2 taken after the low temperature measurements(b)

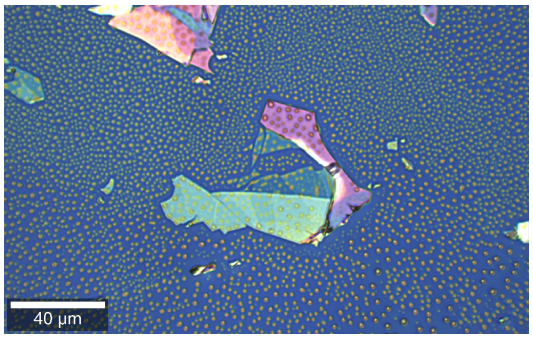

Figure 16: Sample at 173 K showing clumps at the surface.

6 Conclusion

In conclusion, we took photoluminescence (PL) measurements of 2D tungstendisulfide (WS_2) at temperatures between 293 K and 83 K to find the temperature dependence of the exciton resonance.
First we exfoliated some WS_2 flakes and stamped them on a Si/SiO_2 substrate. Then we characterized the sample using PL measurements with a 532 nm laser to find which area is monolayer, and using Raman spectra to confirm that the sample is WS_2 on a Si/SiO_2 substrate. Lastly, using reflectance measurements to measure excitons in the bulk. The characterization showed that we had found the right sample and it also showed strong exciton peaks, although these became significantly smaller during the low temperature measurements.
After this we placed the sample in a vacuum and performed low temperature measurements using liquid nitrogen for cooling. After fitting the data we find that the peak positions for both excitons and trions approximately is well described by the Varshni equation. Despite the fact that this equation is normally used for 3D crystals, it can still be used for 2D crystal if we use different constants. Besides this we also measured the FWHM and fitted it according to the Fröhlich interaction, but this did not match theory due to imperfections in the measuring setup.

6.1 Future experiments and outlook

This experiment can be improved upon by creating a setup wherein the sample doesn't move and the vacuum is better. Besides this, we could also take more datapoints and accumulations to improve the accuracy of the fits. Another way to improve this experiment is by using liquid helium, because with liquid helium it becomes possible for the sample to reach a temperature of 4.15 K [19] which is preferable because these temperatures would most likely cause stronger exciton resonances.
Future experiments can use the data from this experiment to calculate the temperature dependence of the exciton resonance for lower temperatures.

References

[1] Tom Hoekstra. 2D WS_2 Photodetectors for Excitonic Light Absorption (2021).

[2] Cong, Chunxiao, et al. "Optical properties of 2D semiconductor WS_2." Advanced Optical Materials 6.1 (2018): 1700767.

[3] Terrones, Humberto López-Urías, Florentino Terrones, Mauricio. (2013). Novel hetero-layered materials with tunable direct band gaps by sandwiching different metal disulfides and diselenides. Scientific reports. 3. 1549. 10.1038/srep01549.

[4] Fox, M. (2002). Optical properties of solids.

[5] Martin Pumera, Adeline Huiling Loo, Layered transition-metal dichalcogenides (MoS_2 and WS_2) for sensing and biosensing, TrAC Trends in Analytical Chemistry, Volume 61, 2014, Pages 49-53

[6] Chakraborty, Biswanath, et al. "Control of strong light–matter interaction in monolayer WS2 through electric field gating." Nano letters 18.10 (2018): 6455-6460.

[7] McCreary, Kathleen M., et al. "A-and B-exciton photoluminescence intensity ratio as a measure of sample quality for transition metal dichalcogenide monolayers." Apl Materials 6.11 (2018): 111106.

[8] Ross, Jason S., et al. "Electrical control of neutral and charged excitons in a monolayer semiconductor." Nature communications 4.1 (2013): 1-6.

[9] Hernandez Martinez, Pedro. (2010). Optical properties of nanoparticles and nanowires: Exciton-plasmon interaction and photo-thermal effects.

[10] Campion, Alan, and Patanjali Kambhampati. "Surface-enhanced Raman scattering." Chemical society reviews 27.4 (1998): 241-250.

[11] Liu Kunxiang et all, Raman Spectroscopy: A Novel Technology for Gastric Cancer Diagnosis, Frontiers in Bioengineering and Biotechnology, volume 10, (2022)

[12] Rudin, S., T. L. Reinecke, and B. Segall. "Temperature-dependent exciton linewidths in semiconductors." Physical Review B 42.17 (1990): 11218.

[13] Sakthivel, P., Muthukumaran, S. Ashokkumar, M. Structural, band gap and photoluminescence behaviour of Mn-doped ZnS quantum dots annealed under Ar atmosphere. J Mater Sci: Mater Electron 26, 1533–1542 (2015).

[14] Plechinger, Gerd, et al. "Identification of excitons, trions and biexcitons in single-layer WS_2." physica status solidi (RRL)–Rapid Research Letters 9.8 (2015): 457-461.

[15] Qiao, Shuai, et al. "Identifying the number of WS_2 layers via Raman and photoluminescence spectrum." 2017 5th International Conference on Mechatronics, Materials, Chemistry and Computer Engineering (ICMMCCE 2017). Atlantis Press, 2017.

[16] Wang, X. H., et al. "Photoinduced doping and photoluminescence signature in an exfoliated WS_2 monolayer semiconductor." RSC advances 6.33 (2016): 27677-27681.

[17] Li, Xiaoli, et al. "Layer-number dependent reflection spectra of WS_2 and WSe_2 flakes on SiO_2/Si substrate." 2017 International Conference on Optical Instruments and Technology: Optoelectronic Measurement Technology and Systems. Vol. 10621. SPIE, 2018.

[18] Niu, Yue, et al. "Thickness-dependent differential reflectance spectra of monolayer and few-layer MoS_2, $MoSe_2$, WS_2 and WSe_2." Nanomaterials 8.9 (2018): 725.

[19] "The Observed Properties of Liquid Helium at the Saturated Vapor Pressure". University of Oregon. 2004.